www.DeepakPublishing.com

Rawashdeh, S. et al. (2016): JoSS, Vol. 5, No. 2, pp. 457–466
(Peer-reviewed article available at www.jossonline.com)

www. JoSSonline.com

Solar Simulator for Spacecraft Photovoltaic Power System Hardware-in-the-Loop Testing

Samir A. Rawashdeh
University of Michigan, Dearborn, MI USA

Mark Simonds and James E. Lumpp
University of Kentucky, Lexington, KY USA

Valdis Zeps
Bluegrass Community and Technical College, Lexington, KY USA

Abstract

To calculate the necessary power requirements for a CubeSat in orbit, designers must estimate the solar exposure to individual solar panels mounted on the CubeSat exterior as a function of its attitude relative to the Sun. To ensure that power generation never falls below minimum requirements, conservative estimates are usually given, leading to excess hardware and lost energy. Developing a system to simulate solar exposure on the solar cell arrays of a CubeSat would allow the accurate calculation of the power generated by each solar panel as the CubeSat propagates through orbit. Therefore, it would be possible to accurately estimate the generated power of the whole system at any given time and position in orbit. The simulation system consists of two components, a solar simulation booth that will project an emulated solar spectrum onto a solar array, and software that can accurately simulate the attitude and trajectory of the CubeSat in orbit. The solar simulation booth will use high powered LEDs and halogen lamps to emulate the portion of the solar spectrum that triple junction solar cells have typically used on CubeSats to generate power. The system is designed to be controllable by spacecraft attitude simulators to perform hardware-in-the-loop simulations.

Corresponding Author: Samir Rawashdeh, rawashdeh@umich.edu
Publication History: Submitted – 08/24/15; Revision Accepted – 05/25/16; Published – 06/15/16

1. Introduction

Small spacecraft, particularly CubeSats, face power generation challenges in orbit because of the limited surface area available for solar panels. Figure 1 is a photo of KySat-2, a 1-unit CubeSat (weighing less than 1.3 kg, and measuring 10 x 10 x 10 cm^3 when stowed) that was designed in Kentucky and launched in November 2013. KySat-2 includes deployable side panels (as depicted) to increase the available area for solar cells (Mitchell et al., 2014).

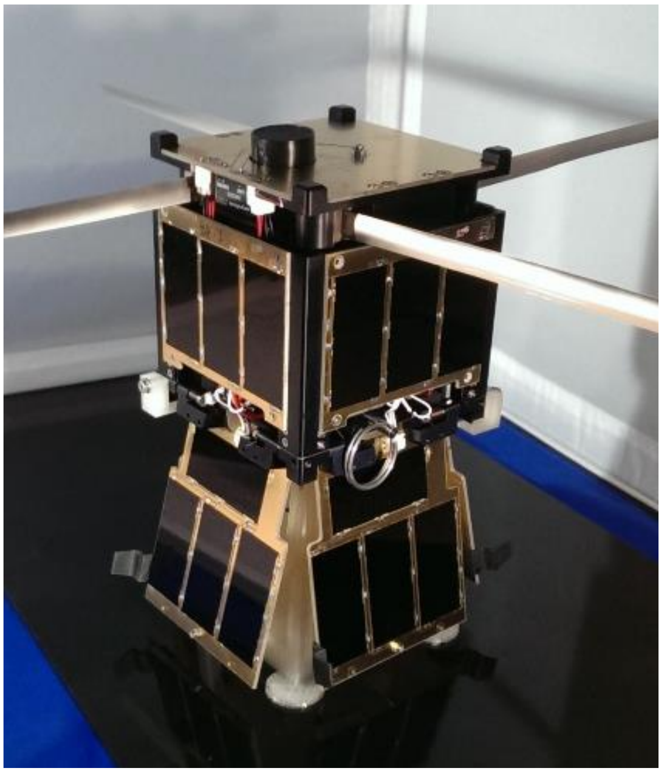

Figure 1. KySat-2 in the deployed configuration.

CubeSat missions, and in particular 1U CubeSats, are typically constrained by the power budget of the CubeSat. Therefore, CubeSat teams seek methods to increase the amount of solar power available through deployable panels, solar cell packing geometries, and experimental solar cells. Typically, teams must rely on mathematical approximations to attempt to determine the on-orbit power generation of a CubeSat. The current integrated system was designed to allow testing of the solar power generation capabilities of a CubeSat, which would provide an improvement over analytical estimates with larger safety margins.

The electric power system (EPS) on a satellite is a critical subsystem that can be considered a singular point of failure, where an EPS failure probably ends the entire mission. Therefore, reliability is a key design and testing factor. This paper presents the design of a solar simulator for a relatively large area that can be used in the design, verification, and testing of spacecraft electric power systems and solar arrays. The objective is to provide a testing platform that helps increase the chance of on-orbit success of a CubeSat. Possible applications include:

Solar Cell Matching when Constructing Solar Arrays

The solar simulator provides a test setup that can be used to generate repeatable measures of individual solar cell I-V characteristics, which is an important step when matching cells to construct larger solar arrays. Electric current ratings should be matched when putting cells in series (to increase operating voltage), and string voltages should be matched when connecting strings in parallel (to boost current capacity). Testing in a simulator helps identify bad cells that do not meet their expected performance and would in turn limit the power generation capability of the entire array. The collective array can be tested as well to verify its operating.

Testing EPS Power Transfer Approaches

When developing solar array interface circuitry (often a maximum power point tracking (MPPT) approach using feedback), solar cells under illumination are the ideal test sources that are closest to the operating environment. The simulator can be used to run illumination profiles emulating rotation relative to the sun to characterize the response of the power-tracking system under these changes, which is an important factor, as discussed in previous work (Erb, Rawashdeh, and Lumpp, 2011). An example in the literature includes a design of an LED-based simulator (using an array of high intensity white LEDs) for maximum power point tracking dynamic response testing (Buso, Spiazzi, and Meneghini, 2013).

End-to-end Power System Testing

An end-to-end test for solar power generation, battery storage, and load management can be used to verify and increase confidence in the system. By running illumination profiles of sun illumination expected in orbit (as described in this paper), an accurate power budget can be constructed that is an improvement over available power estimates. Also, system dynamics can be monitored with sporadic loads (such as radio transmissions) under various illumination conditions. These types of simulations will be beneficial in the design and mission planning stages of a CubeSat mission. Most importantly, the solar booth will help determine the power budgets and mission capabilities during different stages of the satellite's orbit.

This system leverages the capabilities of the Smart Nanosatellite Attitude Propagator (SNAP) (Rawashdeh, 2010) to predict the attitude of CubeSats under various attitude stabilization profiles, in various orbits. SNAP will allow users to calculate the amount of sun exposure one's satellite could receive for a particular attitude profile and orbit. The illumination information as a function of time will be exported to the solar booth controller to simulate the irradiance incident on one of the satellite's faces, by manipulating its lighting to match the estimated solar conditions predicted by SNAP.

2. Related Work

In previous work, the current authors designed a solar simulation booth that used a combination of a halogen light source and a metal-halide lamp to simulate the solar spectrum, similar to the design presented in Guvench et al. (2004). The booth was used in several studies to test solar cells and estimate their properties (Aljoaba, S. Z. et al., 2013; Torabi, Lumpp, J. K., and Lumpp, J. E., 2011). The design shown in this paper incorporates lessons learned from the previous design, which was based on alternating-current (AC) Halogen and Metal-Halide lamps, which are summarized in the design criteria list in the following section.

A number of solar light simulators are discussed in the literature (Wang and Laumert, 2014). Early work achieved good uniformity and irradiance with a set of LEDs (Kohraku and Kurokawa, 2003), and spectral estimates appeared promising, but more thorough analysis was needed. A solid-state solar simulator uses a set of LEDs to simulate the Air Mass AM1.5 spectrum over an area of 10 x 5 cm^2 in the visible light range (Bazzi et al., 2012). Similarly, another LED-based simulator has been developed to provide a spectral match over 22 x 22 cm2 up to 1100nm (Bliss, Betts, and Gottschalg, 2009). Infra-red LEDs have been proposed to improve the spectral match at longer wavelengths (Bazzi et al., 2012). Infra-red illumination is critical to the goal of engaging all junctions of a triple-junction solar cell.

A design based on a set of LEDs and Halogen lamps was designed to cover a 12.5 x 5 cm^2 test area and provide a good spectral match (Grandi and Ienina, 2013). The analysis covered the wavelength range from 400 to 1100 nm, however, targeting silicon-based solar cells for terrestrial use. As discussed in the following section and highlighted in Figure 2, this study's aim was to replicate solar light conditions for a triple-junction solar cell (with wavelength range from 400 to 1600 nm) in space, to test satellite electric power systems.

3. Design Criteria

In designing the light booth, several design criteria influenced the light source selection:

- *Spectrum of Interest.* The light spectrum emitted by the light booth would ideally mimic the solar spectrum exactly, which is however, impractical. For the purposes of power generation testing and simulation, only the part of the spectrum within the solar cell response range needs to be recreated. Figure 2 shows the quantum efficiency plot for the Improved Triple Junction (ITJ) solar cells from Spectrolab Inc.

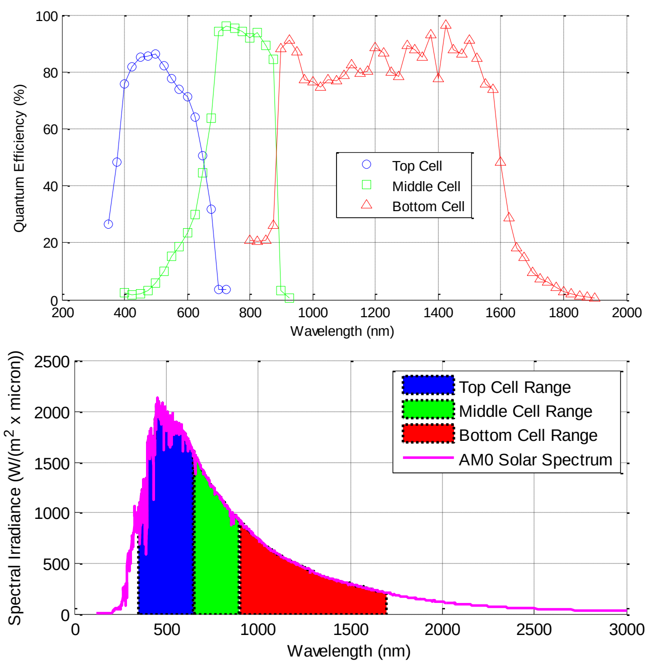

Figure 1. Spectral response of Improved Triple-Junction (ITJ) solar cells of 26.8% efficiency. Top: Quantum Efficiency data courtesy of Spectrolab Inc. Bottom: AM0 Solar spectrum with highlighted response range of each junction. The solar simulator shall approximate the sun's illumination within the 400nm to 1600nm response range.

(2008), which are typically used on Spacecraft. The solar spectrum above the atmosphere, at Air Mass zero (AM0), is shown in relation to the solar cell response range. The American Society for Testing and Materials standard extraterrestrial AM0 reference (ASTM E-490) was used.

- *Controllable Irradiance.* With the goal of simulating on-orbit exposure, the light intensity must be controllable to simulate reduced power generation caused by changes in the sun incidence angle as calculated by the spacecraft attitude simulator. This criteria excludes light sources that are not dimmable.
- *Direct Current (DC) Light.* To test EPS energy transfer and regulation components, the light sources must be "direct" and non-fluctuating, as sunlight is. This criteria excludes light sources with AC power (typical for florescent lights). AC light would place the power system in an unrealistic charging and cutoff cycle and complicate I-V Curve measurements.
- *Large area, low cost, and scalability.* Industrial solar light simulators are cost prohibitive and aim to reproduce solar illumination on a small working area. The booth designed in this work has a working area of 10 cm by 20 cm, the area in the range of a typical CubeSat solar panel, which is significantly larger than most high fidelity simulators. Figure 1 depicts KySat-2, a 10 x 10 x 10 cm^3 satellite with deployable side panels. Each side of KySat-2 when deployed measures 10 x 20 cm^2. The design should be relatively low-cost and scalable to allow expansion to simulate larger solar arrays by replicating the light sources to cover additional surface area.

4. Solar Booth Design

Light Source Selection

Industrial solar light simulators are typically based on Xenon Arc Lamps (Abet Technologies, n/d). However, such equipment is cost prohibitive and aims to reproduce solar illumination on a small working area. The present work experimented with a lower cost automotive set of Xenon lamps. Spectral measurement showed that they reproduce a significant amount of the solar spectrum (near ultraviolet until 850nm). However, the intensity produced per watt of power used was insufficient and number of lamps required would exceed cost and space requirements for the light booth.

Metal-halide lamps were also considered for the light booth, since the intensity and spectrum are favorable. Metal-halide lamps have been used in other designs described in literature (Guvench et al., 2004). However, these lamps run at a fixed intensity and are not typically dimmable, which makes them unfit for our application.

High-intensity 3-Watt LEDs were also tested to evaluate their perspective spectrums. The spectra of the chosen LEDs are shown in a later section, including the red, green, blue, and white LEDs. It was found that a combination of LED colors can be used to reproduce a wide spectrum with control over the shape of the output spectrum. The white LEDs cover most of the visible spectrum, but there is a significant intensity decrease in the 450 nm – 550 nm range that can be compensated for by using the blue and green LEDs.

Alongside high-intensity LEDs, tungsten-halogen lamps were used. These lamps are dimmable, can be run off DC power, and complement the LED spectra by producing longer wavelengths, also shown in Figure 5. This study found that a combination of halogen and high-intensity LEDs can be used to produce wide-spectrum illumination that can be used to test triple-junction solar cells, while engaging all three junctions, illustrated in Figure 2. The halogen lamp spectrum is concentrated in the near infrared (NIR) and IR wavelengths with very high intensity. When the spectra of the blue, green, and white LEDs and the halogen lamp are combined, the complete visible spectrum and a considerable amount of the IR spectrum are reproduced. This motivated the selected light combination. It was noted that the Sun's spectrum in space (AM0), without atmospheric attenuation, extends further into the ultraviolet spectrum. However, the response of the triple-junction solar cells at those wavelengths is limited, due to the quantum efficiency of the GaInP junction below 400 nm being under 40% (Meusel et al., 2003). Thus, the major part of the spectrum to test and simulate the solar panels can be reproduced using the described arrangement of LEDs and halogen lamps.

System Overview

Figure 3 is a block diagram of the solar simulator that was developed. The light booth contains a controllable set of halogen lamps and arrays of high-intensity LEDs. All light sources are running off of DC power (producing DC light) and the intensity is controllable. A current control circuit was developed to control the intensity of the halogen lights. Off-the-shelf LED driver modules were used to control the intensity of the LED arrays. An embedded microcontroller can be commanded to run illumination test profiles or be controlled by a spacecraft simulator emulating the illumination on orbit.

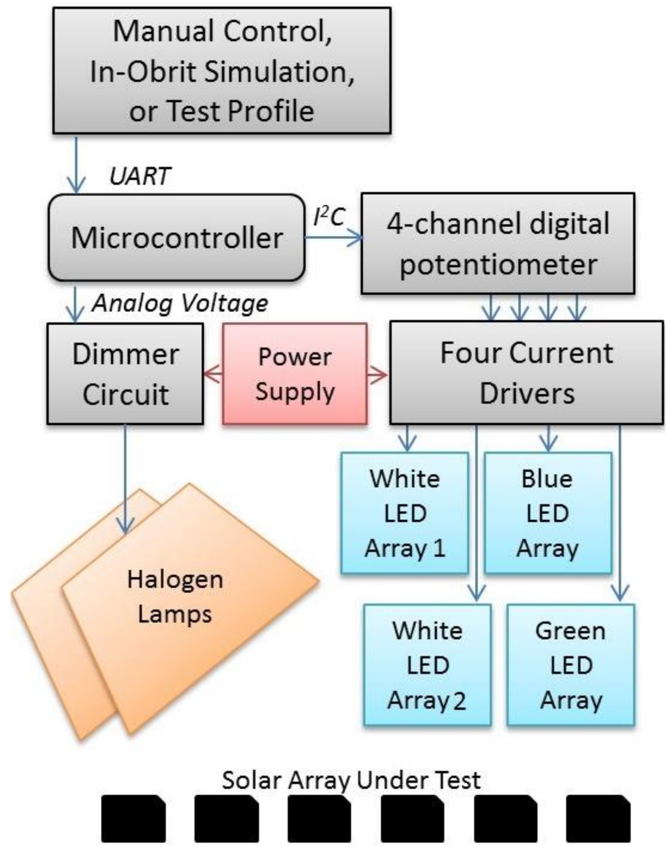

Figure 3. Diagram of solar simulator design. The light booth contains a controllable set of halogen lamps and arrays of high-intensity LEDs.

The microcontroller system receives illumination commands through a Universal Asynchronous Receiver Transmitter (UART) serial connection. Our simulation environment is implemented in Simulink® and has been augmented to transmit the values of the incident angle over UART. The microcontroller then controls the LED array illumination through a set of digital potentiometers controllable using the Inter-Integrated Circuit (I^2C) communication protocol. Also, the internal digital to analog converter subsystem was used to control the halogen lamp dimmer circuit.

Implementation

To identify the number of Halogen lamps and LEDs needed of each color, measurements were made with a lux meter and a sample solar cell. The goal was to include sufficient light sources of each type to reach a full sun's irradiance while having uniform coverage of the area. While the measurement devices may not cover the entire spectrum of interest (such as the lux meter's luminosity function), the goal was to achieve a minimum irradiance. Recalling that all light sources are dimmable, later analysis with a spectrometer can set the relative intensity values to match the solar spectrum shape.

At full power, the blue, green, and white LEDs produced 60, 180 and 180 lux, respectively. Based upon measuring the spectra of the individual light sources of the total approximate 120,000 lux required (the solar illuminance), 90,000 lux were produced by the LEDs and 30,000 Lux were produced by the halogen lamps. A total of 30 white, 16 blue, and 8 green LEDs were assembled into an array, as shown in Figure 4. To focus the intensity produced by the LEDs

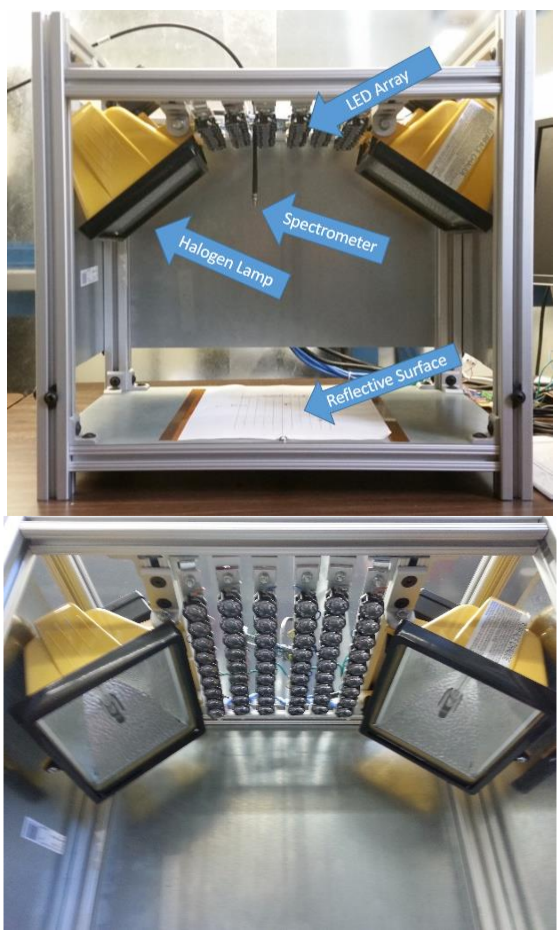

Figure 4. Photos of implemented solar booth and test setup.

onto the exposure area, 8° clear spotlight lenses were used. These lenses provided for good concentration while maintaining an appropriate uniformity throughout the exposure area.

Two halogen lamps were fixed to the booth, one on each side of the LED array and focused onto the exposure area. The intensity of both halogen lamps was controlled simultaneously through a dimming circuit, which is essentially a variable shunt resistor. The LEDs were grouped into green, blue, and white channels. These three channels were independently controlled by the microcontroller via off-the-shelf LED current drivers.

The intensity of the halogen and three LED channels were tuned until the measured irradiance spectrum matched that of the solar spectrum. This was considered 'full irradiance.' Next was the task of being able to dim this maximum irradiance value to simulate different irradiances throughout the satellite's orbit. The four channels could not simply be dimmed in unison because their intensities had a non-linear relationship. Each channel had to be dimmed independently until they matched the dimmed solar spectrum, leading to the characterization of each channel as a function of solar spectrum irradiance. After this was completed, a simple value between 0 and 100 could be sent to the microcontroller, which resulted in a simulated solar spectrum of intensity between 0% and 100%.

5. Characterization Results

Spectrum

A spectrometer (Exemplar LS BRC115U) was used throughout the work to evaluate candidate light sources and find a light combination to match the sun spectrum as closely as possible in the response range of triple-junction solar cells. The measured LED and Halogen spectra are shown in Figure 5.

The measurements underwent a correction for two factors. First, when measuring the solar spectrum comparing it to the theoretical expected value, it was found that the spectrometer did not have a flat response as a function of wavelength throughout the range. Mainly, the sensitivity tapered off near the edges of the response window. Second, the majority of the measurements were taken of scattered light off of

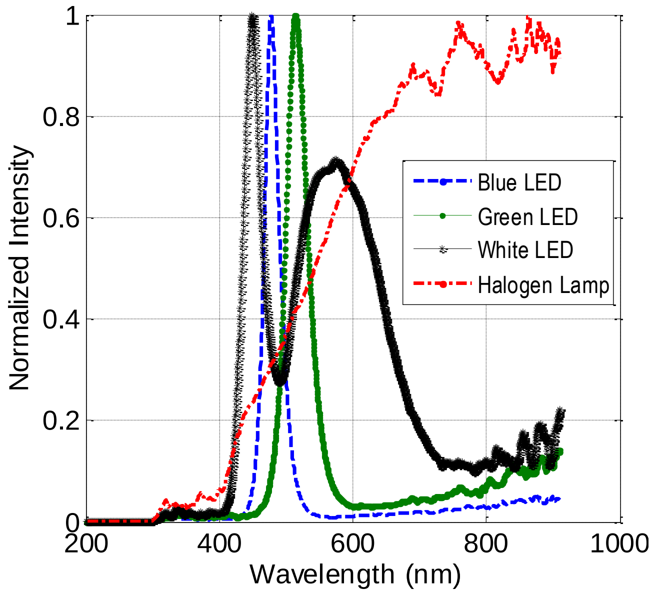

Figure 5. Normalized spectra of individual light sources used.

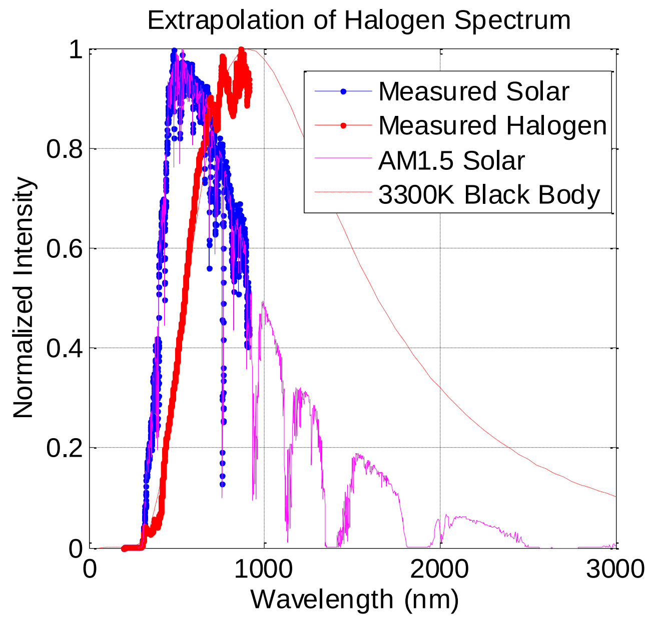

Figure 6. Spectrometer reading correction and black-body extrapolation of halogen lamp spectrum.

a white sheet of paper. This was done because the spectrometer aperture was very narrow, and it was impossible to observe the resulting spectrum of multiple light sources without having them all scatter off of a common surface. The white paper does not reflect all wavelengths at the same magnitude, and the measurements in turn needed correction.

To correct for the spectrometer sensitivity and reflection functions, the spectrum of the sun (reflected off of a white sheet of paper) was measured and compared to reference AM1.5 (Air Mass 1.5) spectrum of the American Society for Testing and Materials (ASTM) (2003). A correction factor as a function of wavelength was calculated to correct the measured solar spectrum to match the established reference, as shown in Figure 6. The correction factor was used to correct all other measurements of reflected light off of a white sheet of paper. The correction factor is essentially parabolic, where it amplifies measurements at the lower and upper wavelength limits of the spectrometer, with more aggressive amplification in the infra-red, where the white paper did not reflect long wavelengths effectively, as expected. Confidence in this correction method was gained when the corrected halogen spectrum matched the theoretically expected shape, as shown in Figure 6, where the spectrum of a tungsten-halogen bulb can be approximated as a black body radiator at around 3300 Kelvin.

Another challenge was that the range of interest is from 400nm to 1400nm, the response range of a triple-junction solar array, while the spectrometer range only spans 300nm to 900nm. This provides an adequate lower limit but ends short in the infra-red. In the absence of a wider range spectrometer, this was addressed by extrapolating the measured spectra into the infra-red. The LED arrays were not expected to illuminate significantly in infra-red. The halogen lights are the only sources with significant illumination at long wavelengths. Therefore, when estimating the spectrum of the combined lights, the LED measured spectra were used to the upper limit of the spectrometer, and the halogen spectrum was approximated by replacing it with a black-body radiator model to extend into the infra-red.

Figure 7 shows the result of tuning the intensity of the individual light sources for a best match of the sun spectrum in space (AM0). Tuning was done initially using an exhaustive search in software, where light source intensity combinations where evaluated relative to the target spectrum. The optimum ratios found where later implemented on the hardware and checked for consistency. The booth provides a good

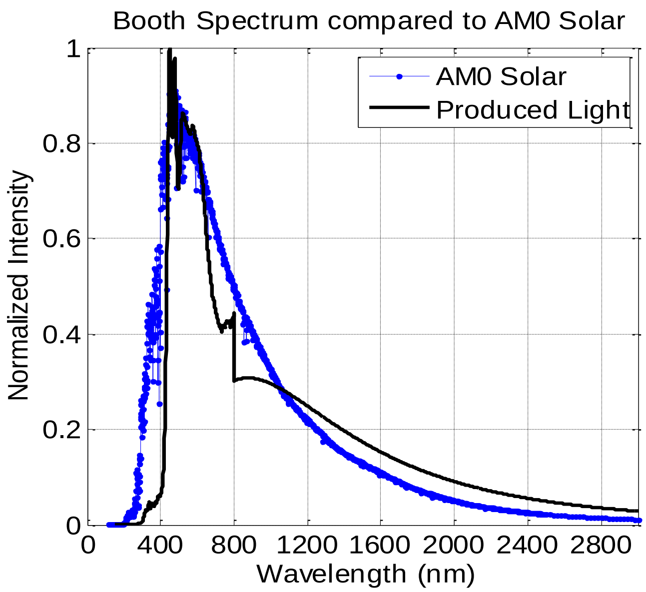

Figure 7. Generated light spectrum compared to the Sun spectrum in space (AM0). The generated light includes high-intensity arrays of white, blue, and green LEDs, and tungsten-halogen lights. The intensity of each light source is tuned for a best match.

spectral match, especially in the range of interest. The highlighted notch shows the spectrometer upper limit. In reality, it is expected that the LED sources (whose spectra were not extrapolated) would indeed emit some light in infra-red and result in a more continuous roll-off function.

Irradiance

After tuning the individual light intensities to produce the spectral match shown in Figure 7, illumination inside the booth was measured to be 140,000 Lux, at full intensity. The solar illuminance constant (without any atmospheric extinction) is 128,000 Lux. This experiment using a standard lux meter provided confidence that the illumination irradiance is in range. The attenuation control can now be used to emulation the sun at different incidence angles.

Uniformity

To evaluate the illumination uniformity, a measurement "pixel" was constructed from an ITJ solar cell, which has the frequency response of interest as discussed previously. A square area measuring one square centimeter was exposed and the short-circuit current was measured at each position inside the booth. Scanning the measurement cell in the 10 cm by 20 cm test area in increments of 1 cm results in a measurement of illumination uniformity shown in Figure 8. The uniformity had a standard deviation of 7.7% around the mean illumination.

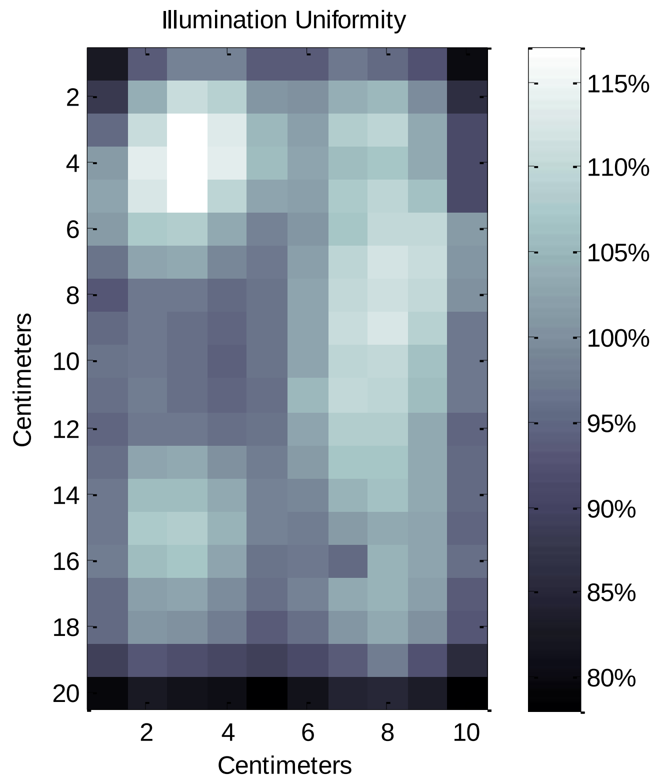

Figure 8. Measured illumination uniformity. Mean illumination is shown as 100%, the illumination standard deviation was 7.7%.

6. Discussion

The intended application of the booth development was to replicate the conditions that a triple junction solar cell would see in space. In this case, the wavelengths of interest span 400nm to 1600nm, and the reference spectrum is sunlight above the atmosphere (the AM0 reference spectrum, no atmospheric mass). To evaluate how well the solar simulator matches the solar spectrum, a spectral match was calculated by estimating the error as the area under the curve of the difference between the produced and desired spectra over the wavelength range of interest. The spectral match was calculated as:

$$Spectral\ Match = \left[1 - \frac{\int_{400}^{1600} |Booth(\lambda) - AM0(\lambda)|\ \partial\lambda}{\int_{400}^{1600} AM0(\lambda)\ \partial\lambda}\right]$$

$$= 80.3\%$$

where *Booth(λ)* is the solar simulator's light spectrum, as shown in Figure 7, and *AM0(λ)* is the solar spectrum in space (at 0 atmospheric mass). For this evaluation of the closeness of the two spectra, the spectra were normalized. The spectral match over this wavelength range is 80.3%.

The spectral match for terrestrial use was evaluated as well. Silicon solar cells with a spectral response between 400nm and 1100nm are typically used. The reference spectrum in this case is the AM1.5 spectrum. A spectral match was calculated as:

$$Spectral\ Match = \left[1 - \frac{\int_{400}^{1100} |Booth(\lambda) - AM1.5(\lambda)|\ \partial\lambda}{\int_{400}^{1100} AM1.5(\lambda)\ \partial\lambda}\right]$$

$$= 82.5\%$$

where *Booth(λ)* is the solar simulator's light spectrum, shown in Figure 7, and *AM1.5(λ)* is the solar spectrum at 1.5 Air Mass. The spectral match over this wavelength range is 82.5%.

It was noted that these two estimates are considered worst-case, where the discontinuity previously discussed and highlighted in Figure 7 contributes to the error in the spectral match estimates. Therefore, uniformity greater than the values calculated can be expected.

The developed booth uses off-the-shelf components at a lower cost compared to commercially available instruments. Solar simulators used in photovoltaics and solar cell characterization typically produce a higher spectral match using specialized lamps and filters, which drives the cost. These precision simulators often illuminate a significantly smaller surface area compared to this study's needs. The current simulation booth achieves a lower but usable spectral match, at a low cost, and over a large surface area. This feature combination is not available commercially.

7. Conclusions

A controllable solar simulator has been developed for the purpose of hardware-in-the-loop testing of photovoltaic devices and electric power systems. The reference design presented covers an area of 10 cm x 20 cm, which is sufficient for a typical CubeSat design. The illumination uniformity had a standard deviation of 7.7%. The system can be scaled to cover larger areas. The simulator consists of a set of high intensity LEDs accompanied by tungsten-halogen lamps. A spectral match greater than 80% within the response of improved triple-junction solar cells (400 nm to 1600 nm) was achieved.

Illumination is controllable through a serial connection. Illumination profiles can be generated to simulate varying conditions, such as test patterns, time of day simulations, and others. The intended application entails using the Smart Nanosatellite Attitude Propagator (SNAP) to simulate a satellite's orientation relative to the Sun while in orbit. This allows for a real-time simulation of the illumination a solar array is receiving in orbit, and in turn can be used to test the behavior of the attached solar array interfacing circuit and power system.

Acknowledgments

The authors thank the NASA Kentucky Space Grant Consortium, the SPRITE Laboratory at NASA Marshall Space Flight Center, and Spectrolab Inc.

References

Abet Technologies (n/d): LS 150 Xenon Arc Lamp Source. Available at: http://www.abet-technologies.com/more-products/light-sources. (last accessed May 23, 2014).

Aljoaba, S. Z. et al. (2013): Thermoelectrical Modeling of Wavelength Effects on Photovoltaic Module Performance—Part II: Parameterization, *IEEE J. Photovoltaics*, Vol. 3, No. 3, pp. 1024–37.

American Society for Testing and Materials (ASTM) (2003): Terrestrial Reference Spectra for Photovoltaic Performance Evaluation, Air Mass 1.5: ASTM G173-03 Reference Spectra Derived from SMARTS v. 2.9.2. Available at: http://rredc.nrel.gov/solar/spectra/am1.5/ (last accessed May 12, 2015).

Bazzi, A. M. et al. (2012): Solid-state Solar Simulator, *Industry Applications, IEEE Transactions on*, Vol. 48, No. 4, pp. 1195–202.

Bliss, M., Betts, T. R., and Gottschalg, R. (2009): An LED-based Photovoltaic Measurement System with Variable Spectrum and Flash Speed, *Solar Energy Materials and Solar Cells*, Vol. 93, No. 6, pp. 825–30.

Buso, S., Spiazzi, G., and Meneghini, M. (2013): Laboratory PV generator for MPPT dynamic response testing, in *IEEE Brazilian Power Electronics Conf. (COBEP)*, pp. 563–68.

Erb, D., Rawashdeh, S. A., and Lumpp, J. E. (2011): Evaluation of Solar Array Peak Power Tracking Technologies for CubeSats, in 25th Annu. *AIAA/USU Conf. on Small Satellites*, Logan, UT.

Grandi, G. and Ienina, A. (2013): Analysis and Realization of a Low-cost Hybrid LED-halogen Solar Simulator, *2013 IEEE Int.Conf.on Renewable Energy Research and Applications (ICRERA)*, pp. 794–99.

Guvench, M. G. et al. (2004): Solar Simulator and I-V Measurement System for Large Area Solar Cell Testing, in *Proc. 2004 Am. Soc. Eng. Ed. Annu. Conf. & Expo*.

Kohraku, S. and Kurokawa, K. (2003): New Methods for Solar Cells Measurement by LED Solar Simulator, *Proc. 3rd World Conf. on Photovoltaic Energy Conversion*, Vol. 2, pp. 1977–80.

Meusel, M. et al. (2003): Spectral Response Measurements of Monolithic GaInP/Ga(In)As/Ge Triple-junction Solar Cells: Measurement Artifacts and their Explanation, *Prog.in Photovoltaics: Research and Applications*, Vol. 11, No. 8.

Mitchell, C. et al. (2014): Development of a Modular Command and Data Handling Architecture for CubeSats, in *Proc. IEEE Aerospace Conf.*, Big Sky, MT.

Rawashdeh (2010): Smart Nanosatellite Attitude Propagator (SNAP). Available at: http://sarlab.net/smart-nanosatellite-attitude-propagator-snap/ (last accessed May 2015).

Spectrolab Inc. (2008): 26.8% Improved Triple Junction (ITJ) Solar Cells, 29 4 2008. Available at: www.spectrolab.com. (last accessed May 12, 2015).

Torabi, N. M., Lumpp, J. K., and Lumpp, J. E. (2011): Materials Selection and Processing Techniques for Small Spacecraft Solar Cell Arrays, in *Int. Microelectronics and Packaging Soc. 44th Symp*.

Wang, W. and Laumert, B. (2014): Simulate a *'Sun'for Solar Research: A Literature Review of Solar Simulator Technology*, Stockholm, Sweden: KTH Royal Institute of Technology.

